

## NMR Spectroscopy | Hot Paper |

**New Experimental Insight into the Nature of Metal–Metal Bonds in Digallium Compounds:  $J$  Coupling between Quadrupolar Nuclei**Libor Kobera, Scott A. Southern, Gyandshwar Kumar Rao, Darrin S. Richeson, and David L. Bryce<sup>\*[a]</sup>

**Abstract:** Multiple bonding between atoms is of ongoing fundamental and applied interest. Here, we report a multinuclear ( $^1\text{H}$ ,  $^{13}\text{C}$ , and  $^{71}\text{Ga}$ ) solid-state magnetic resonance spectroscopic study of digallium compounds which have been proposed, albeit somewhat controversially, to contain single, double, and triple Ga–Ga bonds. Of particular relevance to the nature of these bonds, we have carried out two-dimensional  $^{71}\text{Ga}$   $J/D$ -resolved NMR experiments which provide a direct measurement of  $J(^{71}\text{Ga}, ^{71}\text{Ga})$  spin–spin coupling con-

stants across the gallium–gallium bonds. When placed in the context of clear-cut experimental data for analogous singly, doubly, and triply bonded carbon spin pairs or boron spin pairs, the  $^{71}\text{Ga}$  NMR data clearly support the notion of a different bonding paradigm in the gallium systems. Our findings are consistent with an increasing role across the purported gallane–gallene–gallyne series for classical and/or slipped  $\pi$ -type bonding orbitals.

**Introduction**

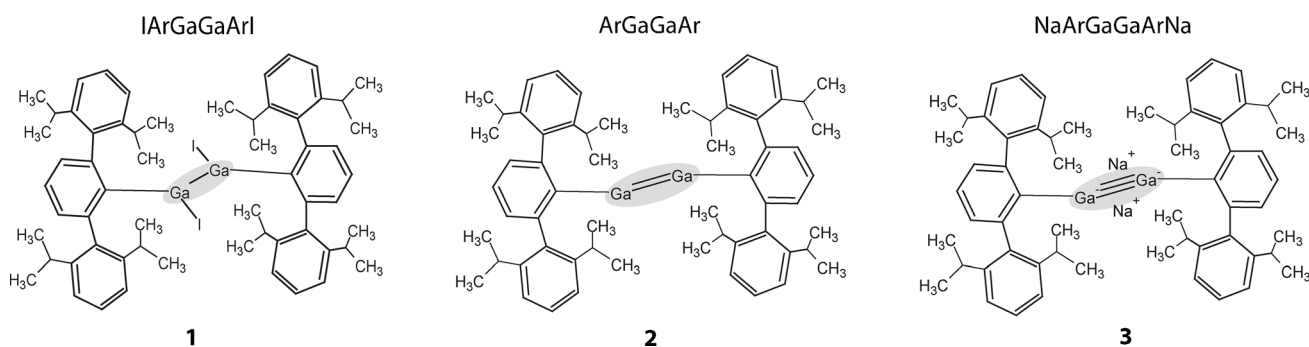
The nature of multiple bonding between elements is a topic of great fundamental and practical interest.<sup>[1–6]</sup> For example, a series of recent papers has provided experimental evidence and a theoretical understanding of the nature of the boron≡boron triple bond.<sup>[7,8]</sup> The excitement around this work is somewhat reminiscent of that generated by the first report by Robinson in 1997 of a gallyne,<sup>[9]</sup> purported to contain a gallium≡gallium triple bond. The description of multiple bonds between gallium atoms has attracted much attention and generated some controversy in the scientific community, with varying conclusions on the nature of Ga–Ga bonding, both in “gallenes” and in “gallynes”. The original gallyne system was stabilized by two sodium ions, and the short Ga–Ga distance of 2.319 Å was a primary argument for the triple bond.<sup>[9]</sup> Subsequently, Klinkhammer proposed, on the basis of a natural bond order analysis, that the gallium–gallium bond in the model system  $\text{HGaGaH}^{2-}$  consists of a  $\sigma$ -bond, a  $\pi$ -bond, and a non-classical “slipped”  $\pi$ -bond,<sup>[10]</sup> and similar conclusions were reached by topographical electron localization function analysis.<sup>[11]</sup> However, Cotton et al. concluded on the basis of density functional theory (DFT) that the gallynes involve only one  $\sigma$ -bond orbital and one  $\pi$ -bonding orbital, along with a nonbonding  $\pi$  orbital, and thus can only be considered as

exhibiting a double bond.<sup>[12]</sup> Robinson and co-workers subsequently carried out calculations on the more realistic complex  $\text{Na}_2[(\text{C}_6\text{H}_5)_2\text{C}_6\text{H}_3\text{GaGaC}_6\text{H}_3(\text{C}_6\text{H}_5)_2]$ <sup>[13,14]</sup> and the claim was made that the nonbonding orbital reported by Cotton et al.<sup>[12]</sup> is actually a bonding orbital, and so the originally reported gallyne should indeed be described as containing a weak triple bond.<sup>[14]</sup> Robinson has further described theoretical models defending this claim, showing that simple compounds such as  $(\text{Me})\text{GaGa}(\text{Me})$  and  $\text{HGaGaH}$ , along with their reduced species, include a weak triple bond comprised of two coordinate bonds and a  $\pi$ -bond.<sup>[15,16]</sup> An experimental study and analysis reported by Power and co-workers in 2002 on  $\text{IArGaGaArI}$  (**1**),  $\text{ArGaGaAr}$  (**2**), and  $\text{NaArGaGaArNa}$  (**3**) [ $\text{Ar} = 2,6\text{-Dipp}_2\text{C}_6\text{H}_3$ ,  $\text{Dipp} = 2,6\text{-}i\text{Pr}_2\text{C}_6\text{H}_3$ ; Scheme 1], however, called into question the bonding order in the purported gallene (**2**) and gallyne (**3**).<sup>[17]</sup> A more recent analysis of the electron localization function concluded that the  $\text{Ga}\equiv\text{Ga}$  bond is a non-classical triple bond consisting of a regular  $\pi$ -bond, a “slipped”  $\pi$ -bond, and a distorted  $\sigma$ -bond.<sup>[18]</sup> The sodium cations were found to contribute greatly to the short Ga–Ga distance and to participate in the  $\pi$ -bond, and it was argued that these compounds should be viewed as comprising  $\text{Ga}_2\text{Na}_2$  clusters.<sup>[18]</sup> An analysis based on domain-averaged Fermi holes of  $(\text{Ph}\text{--}\text{GaGa}\text{--}\text{Ph})\text{Na}_2$  and  $\text{Ph}\text{--}\text{GaGa}\text{--}\text{Ph}^{2-}$  suggested that of the three electron pairs contributing to the  $\text{Ga}\equiv\text{Ga}$  bond, only the  $\pi$ -bond can be considered a classical shared electron pair, while the two other bonds are complex and have partial lone pair character, but cannot be considered fully bonding.<sup>[19]</sup> The previous discussion of gallium–gallium bonding has thus largely focused on X-ray diffraction analyses coupled with computational chemistry and theoretical considerations.

Our laboratory has recently reported the development of a series of  $J$ -resolved solid-state NMR spectroscopy tech-

[a] Dr. L. Kobera, S. A. Southern, Dr. G. K. Rao, Prof. Dr. D. S. Richeson, Prof. Dr. D. L. Bryce  
Department of Chemistry and Biomolecular Sciences and  
Centre for Catalysis Research and Innovation, University of Ottawa  
10 Marie Curie Pvt. D'Iorio Hall, Ottawa, Ontario K1N 6N5 (Canada)  
E-mail: dbryce@uottawa.ca

Supporting information for this article is available on the WWW under  
<http://dx.doi.org/10.1002/chem.201600999>.



**Scheme 1.** Compounds studied in this work. Such compounds have been described as featuring single (1), double (2), and triple (3) gallium–gallium bonds; however, the disputed nature of these bonds is acknowledged by the grey shading.

niques.<sup>[20]</sup> These methods are valuable in that they enable the measurement of indirect nuclear spin-spin ( $J$ ) coupling constants for pairs of quadrupolar nuclei (spin quantum number  $I > 1/2$ ) in the solid state. Such measurements are often impossible in solution due to rapid quadrupolar relaxation of many nuclides of interest. In the solid state, quadrupolar broadening of the line shapes for nuclei such as  $^{11}\text{B}$ ,  $^{71}\text{Ga}$ , (both  $I = 3/2$ ) etc., is often orders of magnitude larger than the  $J$  coupling constant, thereby obscuring the effects of the latter in a standard one-dimensional solid-state NMR (SSNMR) spectrum. Our two-dimensional  $J$ -resolved experiments alleviate these problems and have enabled the measurement of  $J(^{11}\text{B},^{11}\text{B})$  couplings in solid diboranes, diborenes, and diborynes,<sup>[8]</sup> as well as  $J(^{71}\text{Ga},^{71}\text{Ga})$  couplings across single Ga–Ga bonds in  $\text{Ga}_2\text{Cl}_4(\text{dioxane})_2$ ,  $\text{Ga}_2\text{Cl}_4(\text{THP})_2$ , and  $\text{Ga}_2\text{Cl}_4(\text{THF})_2$ .<sup>[21]</sup> The significance of the measurements of these  $J$  couplings arises due to their intimate relationship with the electronic structure of the bond. In the case of multiply bonded boron compounds, we demonstrated a strong correlation between the reduced carbon–carbon coupling constants ( $K = 4\pi^2 J / \gamma_N \gamma_C h$ )<sup>[22]</sup> for alkanes, alkenes, and alkynes with those of diboranes, diborenes, and diborynes, thereby providing key insight into the nature of the boron≡boron triple bond.

The persistent interest and outstanding ambiguity in the description of Ga–Ga bonding prompted us to study this problem via NMR spectroscopy. Specifically, how do the reduced gallium–gallium coupling constants for a gallane–gallene–galline series compare to the values for the well-understood carbon–carbon and boron–boron analogues, and what insight does this provide into the nature of gallium–gallium bonding? Here, we have focused our attention on the preparation and solid-state NMR characterization of a prototypical series of digallium systems which have been proposed to contain single (1), double (2) and triple (3) bonds (Scheme 1). The gallium bonding environments in these compounds have been characterized by  $^1\text{H}$ ,  $^{13}\text{C}$ , and  $^{71}\text{Ga}$  SSNMR spectroscopic methods. In particular, advanced  $^{71}\text{Ga}$   $J$ -resolved NMR techniques<sup>[23,24]</sup> have been applied to overcome issues associated with dipolar and quadrupolar spectral broadening, and homonuclear  $J(^{71}\text{Ga},^{71}\text{Ga})$  couplings have been extracted from the NMR spectra to provide new insights into the nature of gallium–gallium bonds.

## Results and Discussion

### Initial characterization by $^1\text{H}$ and $^{13}\text{C}$ solid-state NMR spectroscopy

Solid-state NMR spectroscopy was used to characterize the digallium compounds. High-resolution  $^1\text{H}$  DUMBO magic-angle spinning (MAS) NMR and  $^{13}\text{C}$  cross-polarization (CP)/MAS NMR experiments were used for primary characterization and the resulting spectra are shown in Figure 1. The assignments of the spectra are based on the literature<sup>[17]</sup> (Table 1).

**Table 1.**  $^1\text{H}$  DUMBO/MAS NMR and  $^{13}\text{C}$  CP/MAS NMR chemical shift assignments for digallium compounds 1, 2, and 3.

Assignment	$^1\text{H}$ NMR (ppm)		
	1	2	3
$\text{CH}_3-$	1.10	1.25	0.95
$>\text{CH}-$	2.58	2.72	2.65
$=\text{CH}- (m-)$	6.92	$\sim 7.46$	$\sim 7.23$
$=\text{CH}- (p-)$	7.71	$\sim 7.46$	$\sim 7.23$
Assignment	$^{13}\text{C}$ NMR (ppm)		
	1	2	3
$\text{CH}_3-$	23.1; 24.3; 25.8; 27.5	24.9	24.7
$>\text{CH}-$	30.2	30.4	30.3
$m\text{-Dipp}$	123.5	122.7	122.8
$p\text{-C}_6\text{H}_3$		128.1	127.8
$i\text{-Dipp}$	130.3		
$m\text{-C}_6\text{H}_3$		128.1	127.8
$o\text{-C}_6\text{H}_3$	139.3	140.0	140.4
$p\text{-Dipp}$	144.9		
$o\text{-Dipp}$	147.9	146.7	146.1
$i\text{-C}_6\text{H}_3$	149.1		

The good resolution of the  $^1\text{H}$  DUMBO/MAS NMR spectrum for 1 allows for clear identification not only of methyl ( $-\text{CH}_3$ ) and methine ( $>\text{CH}-$ ) groups in the aliphatic region of the spectrum, but also the *meta* and *para* protons (Figure 1, left). The  $^{13}\text{C}$  CP/MAS NMR spectrum distinguishes more than twenty individual peaks, which suggests a high degree of crystallinity of compound 1. Both spectra show some impurity peaks which may be attributed to unreacted intermediate product (see Figure 1 and Figure S3 in the Supporting Informa-

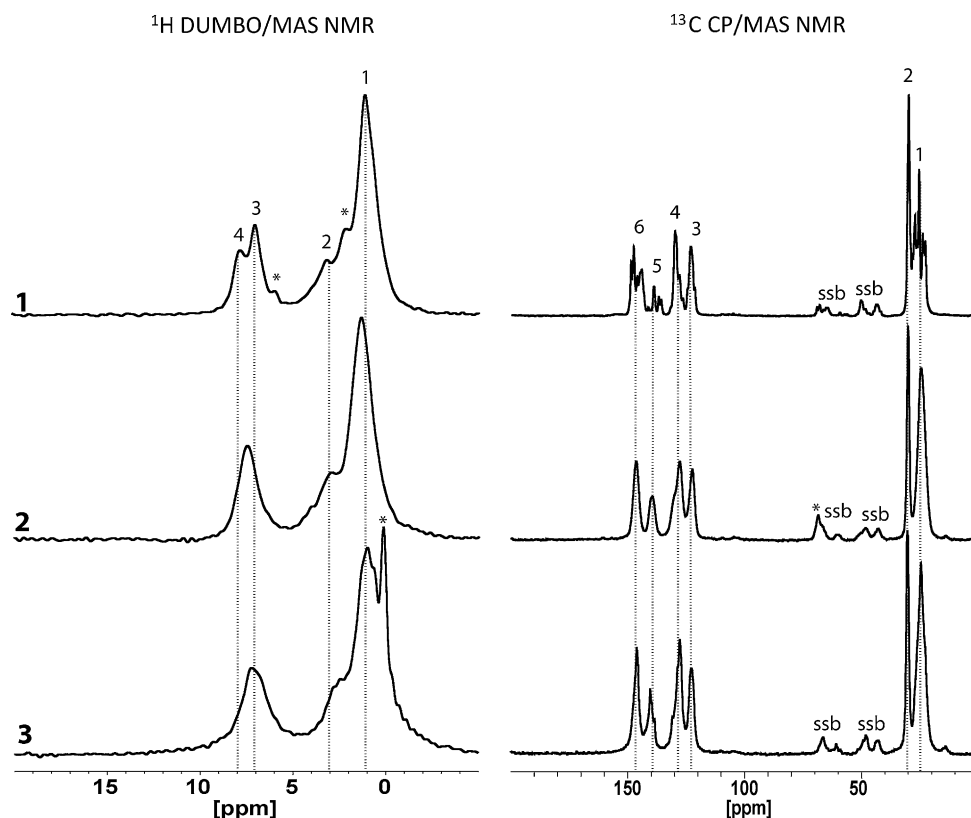


**Figure 1.** Experimental  $^1\text{H}$  DUMBO/MAS NMR spectra collected at 10 kHz MAS (left panel) and  $^{13}\text{C}$  CP/MAS NMR spectra acquired at 8 kHz MAS (right panel) of digallium compounds **1**, **2**, and **3**.  $B_0 = 9.4$  T. Asterisks denote impurities. A regular 4 mm  $\text{ZrO}_2$  rotor was used. Spinning sidebands are indicated by “ssb”.

tion). Some splittings on the order of 100 Hz observed in the  $^{13}\text{C}$  CP/MAS NMR spectra may also be attributed to through-space residual dipolar coupling (RDC) between carbon atoms and the quadrupolar  $^{127}\text{I}$  nuclei ( $I = 5/2$ ).<sup>[25]</sup> (Supporting Information, Figure S3).

The similarity between the  $^1\text{H}$  DUMBO/MAS NMR spectra, and between the  $^{13}\text{C}$  CP/MAS NMR spectra, of the digallium compounds **2** and **3** indicates a comparable degree of overall crystallinity. Additionally, a decreased presence of impurities in **2** and **3** is noted. In the  $^{13}\text{C}$  CP/MAS NMR spectrum of **2**, a small signal at 69 ppm is attributed to residual diethyl ether solvent.<sup>[26]</sup> An impurity at 0.1 ppm is clearly visible in the  $^1\text{H}$  DUMBO/MAS NMR spectrum of system **3**. This impurity can be attributed to the silicone grease used to join reaction flasks during sample preparation.<sup>[26]</sup>

While these spectra provide useful characterization information, they do not provide direct information on the gallium–gallium bond. Therefore, the systems were further investigated by  $^{71}\text{Ga}$  NMR spectroscopy.

### Gallium-71 NMR spectroscopy

Gallium has two NMR-active isotopes,  $^{69}\text{Ga}$  and  $^{71}\text{Ga}$  ( $I = 3/2$ ), with natural abundances of 60.1 and 39.9%, respectively. The less-abundant  $^{71}\text{Ga}$  isotope is observed presently due to its smaller quadrupole moment, which contributes to its higher spectral receptivity relative to  $^{69}\text{Ga}$ .<sup>[27]</sup> Regardless, a strong ap-

plied magnetic field must be used, because both isotopes typically give rise to relatively broad spectral lines, often covering hundreds of ppm.<sup>[21,27]</sup> For nuclei with large quadrupolar interactions, the static quadrupolar Carr–Purcell–Meiboom–Gill (QCPMG) experiment, or a modification thereof (wideband uniform-rate smooth truncation (WURST)-QCPMG) are often advantageous.<sup>[28–30]</sup> For compounds **1** to **3**, it was found that fast  $T_2(^{71}\text{Ga})$  relaxation rendered these experiments impractical. Instead, regular  $^{71}\text{Ga}$  spin-echo NMR experiments were carried out at 21.1 T (Figure 2). The line shapes are largely due to the  $^{71}\text{Ga}$  nuclear electric quadrupolar interaction between the gallium quadrupole moment and the electric field gradient (EFG). In principle, the spectra are also influenced by gallium chemical shift anisotropy (CSA); however, the impact of CSA is expected to be small relative to the dominant quadrupolar coupling and, as such, the spectra were fit only on the basis of the quadrupolar interaction and an isotropic chemical shift. The resulting NMR parameters are listed in Table 2. Errors were determined on an iterative heuristic basis, but then increased to account for our neglect of small CSA effects.

Typical gallium isotropic chemical shifts range from  $-700$  to  $700$  ppm with respect to aqueous  $\text{Ga}_2(\text{NO}_3)_3$ , reflective of the oxidation state and coordination geometry.<sup>[27]</sup> Chemical shifts for  $\text{Ga}^{\text{I}}$  range from  $-700$  to  $0$  ppm, those for  $\text{Ga}^{\text{II}}$  from  $200$  to  $250$  ppm, and from  $0$  to  $700$  ppm for  $\text{Ga}^{\text{III}}$ .<sup>[21,27]</sup> Additionally, a strong correlation between  $^{27}\text{Al}$  NMR and  $^{71}\text{Ga}$  NMR chemical shifts of gallium and aluminum oxides, silicates or phosphates

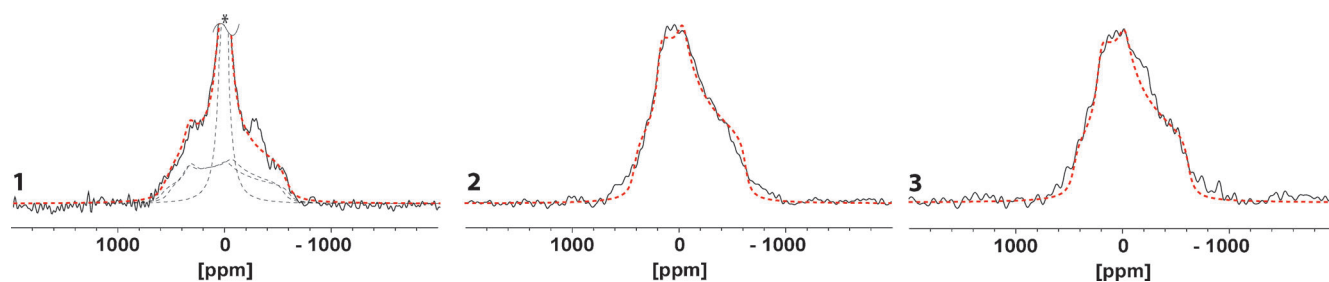


**Figure 2.**  $^{71}\text{Ga}$  spin-echo spectra of static powdered digallium compounds **1**, **2**, and **3**. Experimental data, solid lines; simulated data, dashed lines. The asterisk denotes an impurity resonance in **1**.

**Table 2.**  $^{71}\text{Ga}$  NMR parameters and structural information for the Ga–Ga spin pairs in digallium compounds **1**, **2**, and **3**.<sup>[a]</sup>

Cmpd <sup>[b]</sup>	Site	$\delta_{\text{iso}}$ [ppm]	$C_Q$ [MHz]	$\eta$	$r_{\text{GaGa}}$ [Å]	Spin system	Space group	CCDC number
<b>1</b>	Ga(1)	$200 \pm 50$	$21.2 \pm 1$	$0.60 \pm 0.1$	2.493	AX	$P2_1/c$	186154
	Ga(2)	$180 \pm 50$	$20.5 \pm 1$	$0.52 \pm 0.1$	2.493	AX		
<b>2</b>	Ga	$66 \pm 50$	$19.0 \pm 1$	$0.74 \pm 0.1$	2.627	$A_2$	$P\bar{1}$	186153
<b>3</b>	Ga	$95 \pm 50$	$19.3 \pm 1$	$0.72 \pm 0.1$	2.347	$A_2$	$P2_1/n$	186155

[a]  $C_Q = eV_{33}Q/h$  and  $\eta = (V_{11} - V_{22})/V_{33}$ , where  $Q$  is the nuclear electric quadrupole moment, and  $V_{11}$ ,  $V_{22}$ , and  $V_{33}$  are the principal components of the electric field gradient tensor. [b] NMR parameters of the impurity (unreacted intermediate product) in **1**:  $\delta_{\text{iso}} = 35(\pm 20)$  ppm;  $C_Q = 3.6(\pm 0.5)$  MHz;  $\eta < 0.1$ .

can be seen.<sup>[31,32]</sup> Generally,  $^{27}\text{Al}$  chemical shifts correspond with Al–O environments: for 4-coordinate Al the chemical shift ranges from 50 to 80 ppm, the chemical shift range of 5-coordinated Al is about 30 to 40 ppm, and 6-coordinated Al shifts range from about  $-10$  to 15 ppm.<sup>[33]</sup> Analogously, the  $^{71}\text{Ga}$  chemical shifts of 4-coordinate Ga sites fall within the range of 90 to 120 ppm, 5-coordinate Ga sites resonate between 0 ppm and 30 ppm, and 6-coordinate Ga sites fall between  $-60$  and 10 ppm.<sup>[27,31,32]</sup> The Ga coordination also has a direct influence on the quadrupolar interaction and this trend is observed with  $^{71}\text{Ga}$  in a wide range of inorganic compounds. The  $^{71}\text{Ga}$  quadrupolar coupling constants ( $C_Q$ ) of various gallium oxides in tetra-, penta-, and hexagonal coordination environments range from a few MHz up to 17 MHz.<sup>[34]</sup> However, in our case, as well as in previous work,<sup>[21]</sup>  $C_Q$  reaches values exceeding 19 MHz, which is indicative of the increasing magnitude of the EFG, consistent with asymmetric gallium environments in the digallium systems. These compounds also exhibit unexpected chemical shift values which fall outside of the traditional regions for these coordination environments.<sup>[27,31–33]</sup>

The similar chemical shifts and the quadrupolar parameters for both crystallographically distinct gallium sites of compound **1** (Table 2) suggest the existence of an asymmetric planar (C–Ga–Ga–C) core with a formal Ga<sup>II</sup> oxidation state.<sup>[21,35]</sup> The NMR parameters of the impurity ( $C_Q = 3.6$  MHz,  $\eta_Q = 0$  and  $\delta_{\text{iso}} = 35$  ppm) are indicative of the presence of a mononuclear Ga<sup>III</sup> site in a pseudo-octahedral coordination environment.<sup>[36]</sup> The chemical shift and relatively large  $C_Q$  of systems **2** and **3** sug-

gest a planar, *trans*-bent (C–Ga–Ga–C) core geometry with an oxidation state of +1. The chemical shift values and large values of  $C_Q$  and  $\eta$  can be explained by structural asymmetry along the Ga–Ga bond.

The aforementioned  $^{71}\text{Ga}$  NMR spectra provide useful information about the oxidation states and the coordination environments of each of the gallium sites, but they do not provide direct proof of Ga–Ga bonding nor the bond order. Direct examination of the Ga–Ga bond was carried out using shifted-echo two-dimensional  $J/D$ -resolved NMR experiments, which allow for deep insight into the nature of Ga–Ga bonds (Figure 3). These experiments are quite challenging on these systems due to the dominant quadrupolar broadening of the spectra. In addition, fast  $T_2$  relaxation led to a complete loss of the Ga signal when using a double-quantum filtered version of the experiment. Unfortunately, the unfiltered spectra are affected by a dominant peak at zero frequency. This peak is due in part to spin states which are not affected by  $J$ -modulation during the evolution of the pulse sequence (see references [21] and [23]). Despite this, a simple two-pulse experiment provided sufficient sensitivity and resolution (Figure 3).

In such experiments, we have shown that the  $J$ -splitting magnitude and shape of each doublet component depends intimately on whether or not the quadrupolar spins are related by an inversion center.<sup>[21]</sup> The X-ray crystal structures show that the directly bonded gallium spin pairs are related by an inversion center in compounds **2** and **3** (resulting in  $A_2$  spin systems), but that they are crystallographically and magnetically non-equivalent (AX spin system) in gallane **1** (Table 2).<sup>[17]</sup> Armed with this knowledge, the doublets of the  $^{71}\text{Ga}$   $J$ /

$D$ -resolved spectra may be fitted to extract both the isotropic  $J$  coupling constant and the effective dipolar coupling constant ( $R_{\text{eff}} = R_{\text{DD}} - \Delta J/3$ ). The experimental anisotropic  $J$  coupling ( $\Delta J$ ) can be determined, if the direct dipolar coupling constant,  $R_{\text{DD}}$  (equal to  $(\mu_0 \gamma_1 \gamma_2 \hbar / 4\pi r_{12}^{-3}) / 8\pi^2$ ), is known.<sup>[21]</sup> The effect of  $R_{\text{eff}}$  on the spectra shown in Figure 3 is manifested in the breadth and sense of the powder patterns associated with each component of the doublet.<sup>[21]</sup> The shape of each doublet component is an anisotropic powder pattern with a breadth of  $3R_{\text{eff}}/2$  in the case of the AX spin system (compound **1**), and  $9R_{\text{eff}}/2$  in the case of  $A_2$  spin systems (compounds **2** and **3**).<sup>[21]</sup> Additionally, the sense of these powder patterns is opposite for the  $A_2$  case compared to the AX case. The value of  $J(^{71}\text{Ga}, ^{71}\text{Ga})$  is determined by measuring the difference be-

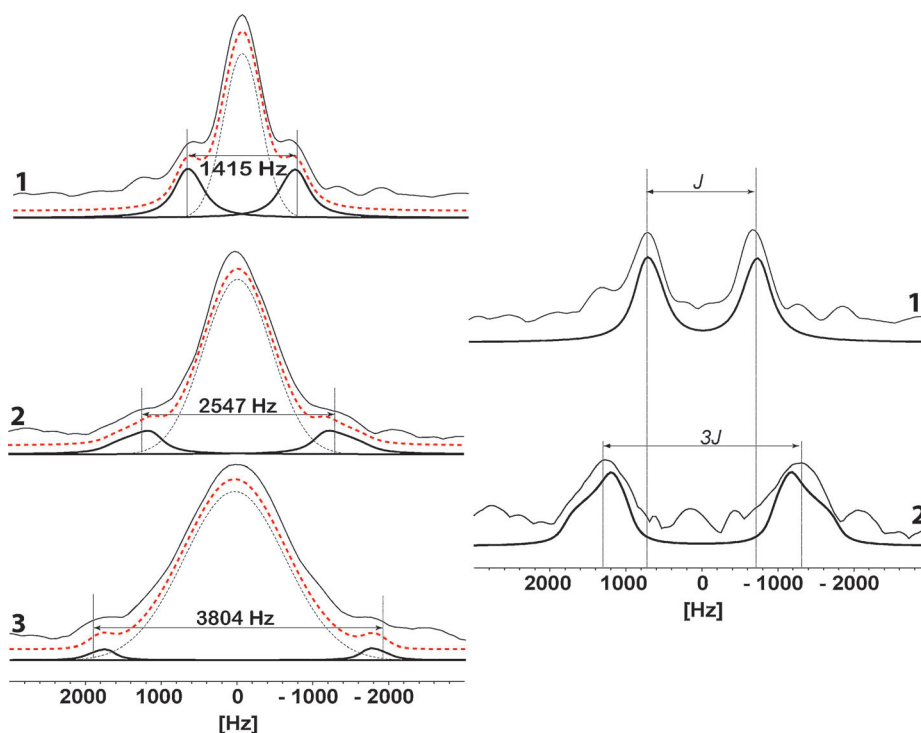


**Figure 3.** Experimental static  $^{71}\text{Ga}$   $J/D$ -resolved NMR (upper) and simulated spectra (red dashed line) of compounds **1**, **2**, and **3** measured at 21.1 T, with determined  $J$  or  $3J$  coupling values (left). On the right are experimental  $^{71}\text{Ga}$   $J/D$ -resolved NMR (upper) and simulated (bottom) spectra after subtracting simulation of the dominant zero-frequency signal.

tween the centers of gravity of each of the two doublet components. In the case of an  $A_2$  spin system (where  $l=3/2$ ), this splitting is equal to three times  $J(^{71}\text{Ga}, ^{71}\text{Ga})$ ; in the AX case, the splitting is directly equal to  $J(^{71}\text{Ga}, ^{71}\text{Ga})$ .<sup>[20,21,23]</sup>

Spectra were fit using two independent methods. First, the raw data sets containing both the zero-frequency peak and the lower-intensity doublets of interest were fit. Second, the zero-frequency peak was removed from the frequency domain through a simple subtraction of a Gaussian peak of appropriate breadth. The resulting doublet spectra were of very good quality for compounds **1** and **2** (Figure 3) and these doublets were also fit directly. The breadth of the zero-frequency peak and low intensity of the doublet peaks for compound **3** precluded the application of the subtraction approach. Nevertheless, the full spectrum for **3** could be fit directly, and special care was taken to ensure the correctness of the fit (Supporting Information, Figure S5).

Several precautions were taken in the fitting of the spectra in Figure 3 to account for the impact of direct dipolar coupling; these have been described previously.<sup>[21]</sup> Briefly, we made the assumption that the effective dipolar coupling constant is relatively insensitive to spectral offset. This is a valid assumption given the moderate overall breadth of the  $^{71}\text{Ga}$  powder patterns and the high values of the quadrupolar asymmetry parameter ( $\eta$ ; far from axial symmetry), as explained in reference [21]. To alleviate concerns about the weakness of the observed doublet peaks as well as their partial overlap with the zero-frequency peak, we acquired the corresponding shifted-echo 2D  $J/D$ -resolved NMR spectrum for a system contain-

ing only monovalent (non-coupled) gallium atoms (Supporting Information, Figure S4); this spectrum shows only a broad zero-frequency peak, with no evidence of doublet structure, as anticipated.

The most well-defined powder patterns are obtained for the doublet components of **2** (perhaps in part due to the absence of nearby  $^{127}\text{I}$  or  $^{23}\text{Na}$  spins which are present for **1** and **3**, respectively), and their sense is consistent with an  $A_2$  spin system (see right-hand panel of Figure 3). The spectrum of **1** was fit using powder patterns of opposite sense to those for **2** and **3**; however, their shape is not well-resolved due to spectral broadening.

The experimental  $J(^{71}\text{Ga}, ^{71}\text{Ga})$  coupling constants are listed in Table 3 and do not show a clear trend with respect to the proposed bond orders for these compounds. This behavior suggests non-classical bonding character (non-traditional multiple bonds) in these systems. The influence of the bond order on the  $J$  coupling constants can be assessed using direct comparisons with experimental data for different spin pairs such as  $^{13}\text{C}-^{13}\text{C}$  or  $^{11}\text{B}-^{11}\text{B}$  in systems where the nature of the bonding is well-established and accepted.<sup>[8]</sup> We have converted the experimental  $J$  coupling constants to reduced coupling constants ( $K$ ), which removes the dependence of the values on nuclide-specific magnetogyric ratios, thereby providing a more suitable parameter for the comparison of differences or similarities in electronic structure between different spin pairs. Several points are worthy of discussion. First, the  $K(^{71}\text{Ga}, ^{71}\text{Ga})$  constants are overall roughly an order of magnitude larger than the  $K(^{13}\text{C}, ^{13}\text{C})$  or  $K(^{11}\text{B}, ^{11}\text{B})$  values, which is in agreement with established

trends for heavier elements.<sup>[22]</sup> Shown in Figure 4b is a plot of the experimental  $K(^{71}\text{Ga}, ^{71}\text{Ga})$  values for **1**, **2**, and **3** versus the experimental  $K(^{13}\text{C}, ^{13}\text{C})$  values for ethane, ethene, and ethyne and also versus the  $K(^{11}\text{B}, ^{11}\text{B})$  values for tetramethyldiborane, a diborene stabilized by two N-heterocyclic carbenes (NHC), and an NHC-stabilized diboryne.<sup>[8]</sup> While there is an excellent linear correlation between the  $K(^{13}\text{C}, ^{13}\text{C})$  and  $K(^{11}\text{B}, ^{11}\text{B})$  values (Figure 4a),<sup>[8]</sup> no such clear correlation exists between the  $K(^{71}\text{Ga}, ^{71}\text{Ga})$  and the  $K(^{13}\text{C}, ^{13}\text{C})$  or  $K(^{11}\text{B}, ^{11}\text{B})$  values, providing a strong indication of a different bonding mechanism in the series of gallium compounds.

**Table 3.** Experimental  $^{71}\text{Ga}, ^{71}\text{Ga}$  spin–spin coupling values for digallium systems.

Cmpd	$R_{\text{DD}}^{\text{[a]}}$ [Hz]	$R_{\text{eff}}^{\text{[b]}}$ [Hz]	$ J_{\text{iso}} ^{\text{[b]}}$ [Hz]	$\Delta J^{\text{[c]}}$ [kHz]
<b>1</b>	728	$465 \pm 50$	$1415 \pm 50$	$0.79 \pm 0.15$
<b>2</b>	618	$168 \pm 50$	$849 \pm 50$	$1.35 \pm 0.15$
<b>3</b>	866	$68 \pm 50$	$1268 \pm 50$	$2.40 \pm 0.15$

[a] Direct dipolar coupling constant calculated from the experimental gallium–gallium distances determined by X-ray diffraction.<sup>[17]</sup> [b] Obtained from spectral fitting. [c] Determination of experimental  $\Delta J$  values was carried out according to  $R_{\text{eff}} = R_{\text{DD}} - \Delta J/3$ , where  $R_{\text{DD}}$  was calculated from the X-ray crystal structures.  $\Delta J = J_{33} - (J_{11} + J_{22})/2$ .

Hardman's crystallographic measurements<sup>[17]</sup> indicate that the bond distances increase in the order  $3 < 1 < 2$  (Table 2); the measured  $J(^{71}\text{Ga}, ^{71}\text{Ga})$  values do not show a clear positive or negative correlation with these distances. This is in contrast to the established dependence of  $J(^{11}\text{B}, ^{11}\text{B})$  on the bond length within a series of  $\sigma$ -bonded diboranes,<sup>[23]</sup> thereby discrediting the possibility that compounds **2** and **3** are held together only by longer or shorter  $\sigma$ -bonds. All of the measured  $J(^{71}\text{Ga}, ^{71}\text{Ga})$  coupling constants are an order of magnitude smaller than those observed previously for the single Ga–Ga bonds in gallium(II) halides stabilized by organoligands.<sup>[21]</sup> This diversity can be induced by mixed oxidation states of gallium (I, III) chlorides combined with different steric shielding<sup>[15]</sup> in comparison with the presently investigated systems.

Given the extensive previous theoretical and computational studies on the nature of multiple gallium–gallium bonds, we prefer not to rely overly on computation in the present work. Nevertheless, in order to understand the nature of gallium–gallium bonds in these digallium systems in more detail, and to corroborate the experimentally measured  $J(^{71}\text{Ga}, ^{71}\text{Ga})$  values, a series of quantum chemical calculations using the B3LYP functional was performed (Supporting Information, Table S1). This method was chosen based on the quality of previously obtained results.<sup>[21]</sup> For compound **1**, the electronic structure of which is the least controversial, excellent agreement is obtained between experimental and computed values ( $1415(\pm 50)$  Hz vs. 1472 Hz). For systems **2** and **3**, discrepancies between the experimental and calculated values of a few hundred Hz are noted; this level of agreement is consistent with a previous report on gallium(II) chlorides stabilized by organoli-

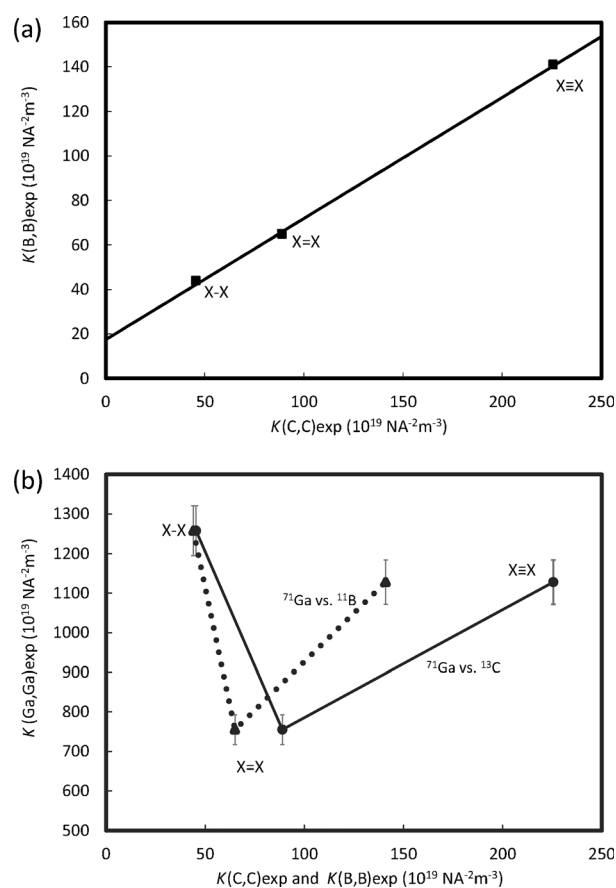


**Figure 4.** a) Correlation between reduced indirect nuclear spin–spin coupling constants ( $K$ ) for B,B spin pairs in  $\text{B}_2\text{Me}_6$ , a NHC-stabilized diborene, and a diboryne, with C,C spin pairs in ethane, ethene, and ethyne, respectively (see reference [8] for further details). b) Correlation between  $K$  for Ga,Ga versus C,C spin pairs (● and solid line) and between Ga,Ga and B,B spin pairs (▲ and dotted line) for **1** (X–X), **2** (X=X), and **3** (X≡X) compounds. The lack of a positive correlation between the data sets in (b) indicates a different electronic structure for the digallium compounds in comparison with the classical  $\sigma/\pi$  model.

gands.<sup>[21]</sup> Nevertheless, the experimentally observed trend is indeed reproduced, that is,  $|J(^{71}\text{Ga}, ^{71}\text{Ga})|$  increases in the order  $2 < 3 < 1$ . Furthermore, the calculations successfully reproduce the experimentally observed order of magnitude difference in the values of  $J(^{71}\text{Ga}, ^{71}\text{Ga})$  for the presently studied compounds ( $\approx 1$  kHz) compared to those reported for the single Ga–Ga bonds in gallium(II) chlorides stabilized by organoligands ( $\approx 10$  kHz).<sup>[21]</sup>

The experimental trend in  $\Delta J(^{71}\text{Ga}, ^{71}\text{Ga})$ , that is,  $1 < 2 < 3$ , is not in concordance with the known experimental trend for  $\Delta J(^{13}\text{C}, ^{13}\text{C})$  for the ethane, ethene, and ethyne series, where the smallest value is noted for ethene and the largest for ethyne.<sup>[37]</sup> This provides further clear evidence for a different electronic structure in the purported gallane–gallene–gallyne systems relative to the prototypical carbon systems. Generally, the anisotropies of the spin–spin coupling tensors report on local symmetry and on the electronic structures of the bonds between the coupled nuclei.<sup>[37–39]</sup> The  $J$  coupling involves the Fermi-contact (FC), spin-orbital (SO), and spin-dipolar (SD) contributions, as well as a  $\text{FC} \times \text{SD}$  cross-term which only contrib-

utes to the anisotropy. The FC interaction is often generated due to covalent bonding between nuclei, mediated by overlapping orbitals with *s* character. The SO contribution reflects the interaction between the magnetic moments of the nuclei and the orbital angular momentum of the surrounding electrons, and may be subdivided into diamagnetic (DSO) and paramagnetic (PSO) parts. A coupling between the nuclear spins and the electronic spins is defined as the SD mechanism.<sup>[37,38]</sup>

In the case of the gallium–gallium bonds, all of our NMR data are consistent with a difference in the electronic structure across the series of compounds **1**, **2**, and **3**, but are clearly inconsistent with a classical  $\sigma/\pi$ -bonding model across this series. The large values of  $|J(^{71}\text{Ga}, ^{71}\text{Ga})|$  for **1** and **3**, which have the shortest gallium–gallium distances, are consistent with a dominant contribution from the FC mechanism and a  $\sigma$ -bond; however, as mentioned, there is no clear correlation between bond length and  $|J(^{71}\text{Ga}, ^{71}\text{Ga})|$  across the full series of three compounds, suggesting that some non-FC mechanisms also play a nontrivial role. This is supported by our DFT calculations, and is in contrast to the case of carbon–carbon bonding where the FC mechanism is overwhelmingly dominant.<sup>[37]</sup> Indeed, our calculations show that the contribution from the PSO term increases substantially in the order  $1 < 2 < 3$  (see the Supporting Information).

The experimental trend observed for  $\Delta J$  clearly indicates a significant contribution from non-FC terms since the FC term is purely isotropic. It is well known that couplings between heavy elements often feature non-FC contributions from the SO and SD mechanisms.<sup>[22,40]</sup> As the paramagnetic SO term is known to be important in bonding situations which do not involve *s*-type orbitals,<sup>[41]</sup> the experimentally observed increase in  $\Delta J$  is consistent with an increased contribution from  $\pi$ -bonding orbitals in the order  $1 < 2 < 3$ .

The participation of sodium anions in the gallium–gallium triple bond<sup>[18]</sup> evokes questions about their arrangement and mobility, because this information may provide an improved understanding of the nature of this multiple bond. The experimental <sup>23</sup>Na MAS NMR spectrum of **3** is depicted in Figure S6 in the Supporting Information. Interestingly, the narrow and relatively symmetric resonance centered at  $-3.25$  ppm may suggest that the Na<sub>2</sub>Ga<sub>2</sub> cluster comprises relatively mobile Na<sup>+</sup> ions.

## Conclusions

In this contribution, we have demonstrated that two-dimensional *J/D*-resolved NMR experiments are powerful tools to measure spin–spin coupling interactions between quadrupolar metal nuclei which give rise to broad spectral lines, including those with fast relaxation times. These experiments provide a new experimental handle on the nature of gallium–gallium bonds. In a prototypical series of digallium compounds, isotropic and anisotropic parts of the  $J(^{71}\text{Ga}, ^{71}\text{Ga})$  coupling tensor were measured and interpreted in the context of analogous <sup>13</sup>C and <sup>11</sup>B NMR data for singly and multiply bonded species featuring carbon–carbon or boron–boron bonds. The experimental values of  $|J(^{71}\text{Ga}, ^{71}\text{Ga})|$  were found to increase in the

order  $2 < 3 < 1$  and this was reproduced by hybrid DFT calculations. The experimental values of  $\Delta J$  increase in the order  $1 < 2 < 3$ . Both of these trends are in disagreement with the known trends for coupling constants in singly, doubly, and triply bonded carbon and boron systems. The  $|J(^{71}\text{Ga}, ^{71}\text{Ga})|$  values also do not correlate simply with the gallium–gallium distances. Taken together, these results uphold the somewhat enigmatic reputation that multiple gallium–gallium bonds have garnered in the literature. While the values of coupling constants in isolation cannot be translated directly into bond orders, the following conclusions are reached: 1) there is significant covalent bonding between pairs of gallium atoms in all three samples; 2) the measured values of  $|J(^{71}\text{Ga}, ^{71}\text{Ga})|$  and  $\Delta J$  show that the electronic structure across the **1**, **2**, **3** series is clearly different from that for related carbon–carbon and boron–boron series; 3) the increase in  $\Delta J$  in the order  $1 < 2 < 3$ , and lack of a straightforward correlation between gallium–gallium bond length and  $J(^{71}\text{Ga}, ^{71}\text{Ga})$ , is consistent with an increased role across the series for classical and/or slipped  $\pi$ -type bonding orbitals, perhaps of the type described by Klinkhammer.<sup>[10]</sup>

## Experimental Section

### Sample preparation

Gal was prepared according to a literature procedure.<sup>[36]</sup> Gal (0.784 g, 4 mmol) in toluene (10 mL) was cooled to  $-78^\circ\text{C}$  using a dry-ice acetone bath. (LiAr)<sub>2</sub> (Ar = 2,6-Dipp<sub>2</sub>C<sub>6</sub>H<sub>3</sub>, Dipp = 2,6-*i*Pr<sub>2</sub>C<sub>6</sub>H<sub>3</sub>) was prepared according to a literature procedure.<sup>[42]</sup> A solution of (LiAr)<sub>2</sub> (1.616 g, 2 mmol) in toluene (20 mL) was added dropwise over a period of 1 h. The mixture was allowed to warm to room temperature over a period of 6 h. The dark green solution was filtered and concentrated to about 10 mL to give a light yellow precipitate. This solution was kept at room temperature for an additional hour and then the precipitate was isolated by decantation. This was then washed with 2 mL hexane and dried to give compound **1** (lArGaGaAr). The dark green liquid was dried to give a red crystalline solid. This was recrystallized from 2 mL of warm hexane to give **2** (ArGaGaAr). A solution of **2** (0.268 g, 0.5 mmol) in diethyl ether (10 mL) was added to sodium metal (0.161 g, 7 mmol) and stirred for 4 h at room temperature. The dark purple solution was filtered to separate the excess sodium. This was concentrated, and cooled in a freezer at  $-20^\circ\text{C}$  for one week to afford a dark red solid (**3**; NaArGaGaArNa). These compounds have been synthesized according to literature procedures.<sup>[17]</sup> The acquired <sup>1</sup>H NMR spectra correspond with the literature data for **1**, **2**, and **3**<sup>[17]</sup> (Supporting information, Figure S1). The prepared samples were stored under inert atmosphere in a glovebox at 277 K.

### Solid-state NMR spectroscopy

Dry powdered samples of **1**, **2**, and **3** were packed into individual ZrO<sub>2</sub> rotors. Solid-state NMR spectra were recorded at 9.4 and 21.1 T using Bruker AVANCE III and Bruker AVANCE II spectrometers, respectively. A 4 mm cross-polarization (CP)/magic angle spinning (MAS) probe was used for <sup>1</sup>H and <sup>13</sup>C experiments at Larmor frequencies of  $\nu(^1\text{H}) = 400.130$  MHz and  $\nu(^{13}\text{C}) = 100.613$  MHz, respectively. The <sup>13</sup>C CP/MAS NMR spectra were collected at 8 kHz and the <sup>1</sup>H DUMBO/MAS NMR spectra were collected at 10 kHz spin-

ning speed. The  $^1\text{H}$  MAS NMR and  $^{13}\text{C}$  MAS NMR isotropic chemical shifts were calibrated with adamantane ( $^1\text{H}$ : 1.85 ppm; central signal) and glycine ( $^{13}\text{C}$ : 176.03 ppm; carbonyl signal) as external standards. A  $^1\text{H}$  DUMBO/MAS NMR set-up experiment on glycine is described and depicted in the Supporting Information, Figure S2.

For  $^{23}\text{Na}$ , a 4 mm CP/MAS probe was used at a Larmor frequency of  $\nu(^{23}\text{Na}) = 105.842$  MHz. A MAS rate of 11 kHz was employed. The  $^{23}\text{Na}$  isotropic chemical shift was calibrated with NaCl(s) as an external standard ( $^{23}\text{Na}$ : 7.2 ppm). The  $\pi/2$  pulse length was 2.1  $\mu\text{s}$  and the recycle delay was 5 s.  $^{71}\text{Ga}$  NMR spectra were collected on stationary samples using a 4 mm CP/MAS probe operating at a Larmor frequency of  $\nu(^{71}\text{Ga}) = 274.510$  MHz ( $B_0 = 21.1$  T). The external standard  $\text{Ga}_2(\text{SO}_4)_3(\text{aq.})$  was used to determine the  $\pi/2$  central transition (CT)-selective pulse as well as for chemical shift calibration ( $^{71}\text{Ga}$ : 0.0 ppm).<sup>[43]</sup> The 2D shifted echo two-pulse  $^{71}\text{Ga}$   $J$ -resolved NMR techniques were developed in our laboratory and evaluated in previous work.<sup>[21]</sup> For the current work, this two-pulse experiment ( $90^\circ_{\text{CT}}-(t_{1/2})-180^\circ_{\text{CT}}-(t_{1/2})-\text{acq.}$ ) was carried out under static conditions at  $B_0 = 21.1$  T. The  $90^\circ_{\text{CT}}$  selective pulse length was 1.2  $\mu\text{s}$  and the recycle delay was 0.5 s. The  $t_1$  evolution period consisted of 32 to 48 increments each consisting of 2048 or 3072 scans, depending on the sample. All NMR experiments were performed at room temperature.

$^{71}\text{Ga}$  NMR spectra of stationary samples were simulated using the "QUAD central" model in the line shape analysis feature of Bruker's Topspin 3.5. CSA was not included in the fits. The simulated  $^{71}\text{Ga}$   $J/D$  resolved spectra were prepared using a superposition of line shapes generated using the "CSA" model in the same software. A manual analysis of the doublet breadths and positions was also used to confirm the parameters obtained through the simulations.

### Quantum chemical calculations

DFT calculations were conducted on models of the three gallium systems. The Cartesian coordinates of the atoms in the models were obtained from the published crystal structures without further optimization (CCDC numbers 186154 (1), 186153 (2), and 186155 (3)).<sup>[17]</sup> To reduce computational requirements, the isopropyl groups were removed and the resulting terminal C–C bonds were replaced with C–H bonds. NMR parameters for each structure were calculated using Gaussian version 2009, rev. D.01.<sup>[44]</sup> The B3LYP functional was used with custom TZP basis sets on all atoms.<sup>[45–48]</sup>

### Acknowledgements

Acknowledgement is made to the donors of The American Chemical Society Petroleum Research Fund for partial support of this research. D.L.B. thanks the Natural Sciences and Engineering Research Council of Canada for funding. We are grateful to Dr. F. A. Perras for valuable discussions. Access to the 21.1 T NMR spectrometer was provided by the National Ultra-high-Field NMR Facility for Solids (Ottawa, Canada), a national research facility funded by a consortium of Canadian Universities, supported by the National Research Council Canada and Bruker BioSpin, and managed by the University of Ottawa (<http://nmr900.ca>).

**Keywords:** gallium · gallyne ·  $J$  coupling · multiple bonding · NMR spectroscopy

- [1] U. Ruschewitz, *Angew. Chem. Int. Ed.* **2016**, *55*, 3264–3266; *Angew. Chem.* **2016**, *128*, 3320–3322.
- [2] Y. Wang, G. H. Robinson, *Chem. Commun.* **2009**, 5201–5213.
- [3] P. P. Power, *J. Chem. Soc. Dalton Trans.* **1998**, 2939–2951.
- [4] a) S. Shaik, D. Danovich, W. Wu, P. Su, H. S. Rzepa, P. C. Hiberty, *Nat. Chem.* **2012**, *4*, 195–200; b) S. Shaik, H. S. Rzepa, R. Hoffmann, *Angew. Chem. Int. Ed.* **2013**, *52*, 3020–3033; *Angew. Chem.* **2013**, *125*, 3094–3109; c) G. Frenking, M. Hermann, *Angew. Chem. Int. Ed.* **2013**, *52*, 5922–5925; *Angew. Chem.* **2013**, *125*, 6036–6039; d) D. Danovich, S. Shaik, H. S. Rzepa, R. Hoffmann, *Angew. Chem. Int. Ed.* **2013**, *52*, 5926–5928; *Angew. Chem.* **2013**, *125*, 6040–6042.
- [5] D. Danovich, P. C. Hiberty, W. Wu, H. S. Rzepa, S. Shaik, *Chem. Eur. J.* **2014**, *20*, 6220–6232.
- [6] *Multiple Bonds Between Metal Atoms* (Eds.: F. A. Cotton, C. A. Murillo, R. A. Walton), Springer, **2005**.
- [7] H. Braunschweig, R. D. Dewhurst, K. Hammond, J. Mies, K. Radacki, A. Vargas, *Science* **2012**, *336*, 1420–1422.
- [8] F. A. Perras, W. C. Ewing, T. Dellermann, J. Böhne, S. Ullrich, T. Schäfer, H. Braunschweig, D. L. Bryce, *Chem. Sci.* **2015**, *6*, 3378–3382.
- [9] J. Su, X.-W. Li, R. C. Crittendon, G. H. Robinson, *J. Am. Chem. Soc.* **1997**, *119*, 5471–5472.
- [10] K. W. Klinkhammer, *Angew. Chem. Int. Ed. Engl.* **1997**, *36*, 2320–2322; *Angew. Chem.* **1997**, *109*, 2414–2416.
- [11] H. Grützmacher, T. F. Fässler, *Chem. Eur. J.* **2000**, *6*, 2317–2325.
- [12] F. A. Cotton, A. H. Cowley, X. Feng, *J. Am. Chem. Soc.* **1998**, *120*, 1795–1799.
- [13] Y. Xie, R. S. Grev, J. Gu, H. F. Schaefer III, P. v. R. Schleyer, J. Su, X.-W. Li, G. H. Robinson, *J. Am. Chem. Soc.* **1998**, *120*, 3773–3780.
- [14] Y. M. Xie, H. F. Schaefer, G. H. Robinson, *Chem. Phys. Lett.* **2000**, *317*, 174–180.
- [15] G. H. Robinson, *Acc. Chem. Res.* **1999**, *32*, 773–782.
- [16] G. H. Robinson, *Chem. Commun.* **2000**, 2175–2181.
- [17] N. J. Hardman, R. J. Wright, A. D. Phillips, P. P. Power, *Angew. Chem. Int. Ed.* **2002**, *41*, 2842–2844; *Angew. Chem.* **2002**, *114*, 2966–2968.
- [18] J. Sun, L. Meng, S. Zheng, Z. Sun, X. Li, *Science China Chemistry* **2012**, *55*, 1370–1376.
- [19] R. Ponec, G. Yuzhakov, X. Gironés, G. Frenking, *Organometallics* **2004**, *23*, 1790–1796.
- [20] F. A. Perras, D. L. Bryce, *eMagRes* **2015**, *4*, 561–574.
- [21] F. A. Perras, D. L. Bryce, *J. Phys. Chem. Lett.* **2014**, *5*, 4049–4054.
- [22] D. L. Bryce, R. E. Wasylshen, J. Autschbach, T. Ziegler, *J. Am. Chem. Soc.* **2002**, *124*, 4894–4900.
- [23] F. A. Perras, D. L. Bryce, *J. Am. Chem. Soc.* **2013**, *135*, 12596–12599.
- [24] F. A. Perras, D. L. Bryce, *Chem. Sci.* **2014**, *5*, 2428–2437.
- [25] V. V. Terskikh, S. J. Lang, P. G. Gordon, G. D. Enright, J. A. Ripmeester, *Magn. Reson. Chem.* **2009**, *47*, 398–406.
- [26] H. E. Gottlieb, V. Kotlyar, A. Nudelman, *J. Org. Chem.* **1997**, *62*, 7512–7515.
- [27] R. E. Wasylshen, S. E. Ashbrook, S. Wimperis, *NMR of Quadrupolar Nuclei in Solid Materials*, Wiley, **2012**.
- [28] J. A. Tang, L. A. O'Dell, P. M. Aguiar, B. E. G. Lucier, D. Sakellariou, R. W. Schurko, *Chem. Phys. Lett.* **2008**, *466*, 227–234.
- [29] L. A. O'Dell, A. J. Rossini, R. W. Schurko, *Chem. Phys. Lett.* **2009**, *468*, 330–335.
- [30] A. W. MacGregor, L. A. O'Dell, R. W. Schurko, *J. Magn. Reson.* **2011**, *208*, 103–113.
- [31] S. M. Bradley, R. F. Howe, R. A. Kydd, *Magn. Reson. Chem.* **1993**, *31*, 883–886.
- [32] J. T. Ash, P. J. Grandinetti, *Magn. Reson. Chem.* **2006**, *44*, 823–831.
- [33] K. J. D. MacKenzie, M. E. Smith, *Multinuclear Solid-State Nuclear Magnetic Resonance of Inorganic Materials*, Pergamon, Amsterdam, **2002**.
- [34] D. Massiot, T. Vosegaard, N. Magneron, D. Trumeau, V. Montouillout, P. Berthet, T. Loiseau, B. Bujoli, *Solid State Nucl. Magn. Reson.* **1999**, *15*, 159–169.
- [35] Z. Černý, J. Macháček, J. Fusek, O. Kříž, B. Čásky, D. G. Tuck, *J. Organomet. Chem.* **1993**, *456*, 25–30.
- [36] C. M. Widdifield, T. Jurca, D. S. Richeson, D. L. Bryce, *Polyhedron* **2012**, *35*, 96–100.
- [37] J. Kaski, P. Lantto, J. Vaara, J. Jokisaari, *J. Am. Chem. Soc.* **1998**, *120*, 3993–4005.

- [38] W. P. Power, M. D. Lumsden, R. E. Wasylishen, *J. Am. Chem. Soc.* **1991**, *113*, 8257–8262.
- [39] M. Kaupp, O. L. Malkina, V. G. Malkin, P. Pyykkö, *Chem. Eur. J.* **1998**, *4*, 118–126.
- [40] D. L. Bryce, R. E. Wasylishen, *Inorg. Chem.* **2002**, *41*, 3091–3101.
- [41] J. Vaara, J. Jokisaari, R. E. Wasylishen, D. L. Bryce, *Prog. Nucl. Magn. Reson. Spectrosc.* **2002**, *41*, 233–304.
- [42] B. Schiemenz, P. P. Power, *Angew. Chem. Int. Ed. Engl.* **1996**, *35*, 2150–2152; *Angew. Chem.* **1996**, *108*, 2288–2290.
- [43] S. M. Bradley, R. A. Kydd, R. Yamdagni, *J. Chem. Soc. Dalton Trans.* **1990**, 413–417.
- [44] Gaussian 09, Revision D.01, M. J. Frisch, G. W. Trucks, H. B. Schlegel, G. E. Scuseria, M. A. Robb, J. R. Cheeseman, G. Scalmani, V. Barone, B. Men-  
nucci, G. A. Petersson, H. Nakatsuji, M. Caricato, X. Li, H. P. Hratchian,  
A. F. Izmaylov, J. Bloino, G. Zheng, J. L. Sonnenberg, M. Hada, M. Ehara,  
K. Toyota, R. Fukuda, J. Hasegawa, M. Ishida, T. Nakajima, Y. Honda, O.  
Kitao, H. Nakai, T. Vreven, J. A. Montgomery, Jr., J. E. Peralta, F. Ogliaro,  
M. Bearpark, J. J. Heyd, E. Brothers, K. N. Kudin, V. N. Staroverov, R. Ko-  
bayashi, J. Normand, K. Raghavachari, A. Rendell, J. C. Burant, S. S. Iyen-  
gar, J. Tomasi, M. Cossi, N. Rega, J. M. Millam, M. Klene, J. E. Knox, J. B.  
Cross, V. Bakken, C. Adamo, J. Jaramillo, R. Gomperts, R. E. Stratmann,  
O. Yazyev, A. J. Austin, R. Cammi, C. Pomelli, J. W. Ochterski, R. L. Martin,  
K. Morokuma, V. G. Zakrzewski, G. A. Voth, P. Salvador, J. J. Dannenberg,  
S. Dapprich, A. D. Daniels, Ö. Farkas, J. B. Foresman, J. V. Ortiz, J. Cio-  
slowski, D. J. Fox, Gaussian Inc., Wallingford, CT, **2009**.
- [45] P. L. Barbieri, P. A. Fantin, F. E. Jorge, *Mol. Phys.* **2006**, *104*, 2945–2954.
- [46] S. F. Machado, G. G. Camiletti, A. Canal Neto, F. E. Jorge, R. S. Jorge, *Mol. Phys.* **2009**, *107*, 1713–1727.
- [47] C. T. Campos, F. E. Jorge, *Mol. Phys.* **2013**, *111*, 167–173.
- [48] a) D. Feller, *J. Comput. Chem.* **1996**, *17*, 1571–1586; b) K. L. Schuchardt,  
B. T. Didier, T. Elsethagen, L. Sun, V. Gurumoorhi, J. Chase, J. Li, T. L.  
Windus, *J. Chem. Inf. Model.* **2007**, *47*, 1045–1052.

Received: March 2, 2016

Published online on ■ ■ ■, 0000

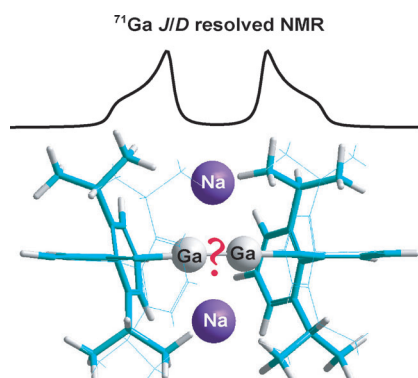
## FULL PAPER

### NMR Spectroscopy

L. Kobera, S. A. Southern, G. K. Rao,  
D. S. Richeson, D. L. Bryce\*



  **New Experimental Insight into the Nature of Metal–Metal Bonds in Digallium Compounds: *J* Coupling between Quadrupolar Nuclei**



**Must be going Ga–Ga:** The nature of gallium–gallium bonding is assessed by measuring  $J(^{71}\text{Ga}, ^{71}\text{Ga})$  coupling constants by solid-state NMR spectroscopy. These experimental data demonstrate that while Ga–Ga systems may feature multiple bonds, their electronic structure clearly differs from that established for analogous carbon–carbon or boron–boron bonds.